ABCG1 influences the brain cholesterol biosynthetic pathway but does not affect amyloid precursor protein or apolipoprotein E metabolism in vivo

Braydon L. Burgess,* Pamela F. Parkinson,* Margaret M. Racke,† Veronica Hirsch-Reinshagen,* Jianjia Fan,* Charmaine Wong,* Sophie Stukas,* Louise Theroux,§ Jeniffer Y. Chan,* James Donkin,* Anna Wilkinson,* Danielle Balik,* Brian Christie, Judes Poirier,§ Dieter Lütjohann,†† Ronald B. DeMattos,† and Cheryl L. Wellington[1,*]**

Department of Pathology and Laboratory Medicine,* Child and Family Research Institute, University of British Columbia, Vancouver, Canada; Lilly Research Laboratories,† Indianapolis, IN; McGill Centre for Studies on Aging,§ Montreal, Canada; Division of Medical Sciences,** University of Victoria, Victoria, Canada; and Department of Clinical Pharmacology,†† University of Bonn, Bonn, Germany

Abstract **Cholesterol homeostasis is of emerging therapeutic importance for Alzheimer's disease (AD). Agonists of liver-X-receptors (LXRs) stimulate several genes that regulate cholesterol homeostasis, and synthetic LXR agonists decrease neuropathological and cognitive phenotypes in AD mouse models. The cholesterol transporter ABCG1 is LXR-responsive and highly expressed in brain. In vitro, conflicting reports exist as to whether ABCG1 promotes or impedes Aβ production. To clarify the in vivo roles of ABCG1 in Aβ metabolism and brain cholesterol homeostasis, we assessed neuropathological and cognitive outcome measures in PDAPP mice expressing excess transgenic ABCG1. A 6-fold increase in ABCG1 levels did not alter Aβ, amyloid, apolipoprotein E levels, cholesterol efflux, or cognitive performance in PDAPP mice. Furthermore, endogenous murine Aβ levels were unchanged in both ABCG1-overexpressing or ABCG1-deficient mice. These data argue against a direct role for ABCG1 in AD. However, excess ABCG1 is associated with decreased levels of sterol precursors and increased levels of SREBP-2 and HMG-CoA-reductase mRNA, whereas deficiency of ABCG1 leads to the opposite effects. Although functions for ABCG1 in cholesterol efflux and Aβ metabolism have been proposed based on results with cellular model systems, the in vivo role of this enigmatic transporter may be largely one of regulating the sterol biosynthetic pathway.**—Burgess, B. L., P. F. Parkinson, M. M. Racke, V. Hirsch-Reinshagen, J. Fan, C. Wong, S. Stukas, L. Theroux, J. Y. Chan, J. Donkin, A. Wilkinson, D. Balik, B. Christie, J. Poirier, D. Lütjohann, R. B. DeMattos, and C. L. Wellington. **ABCG1 influences the brain cholesterol biosynthetic pathway but does not affect amyloid precursor protein or apolipoprotein E metabolism in vivo.** ***J. Lipid Res.*** **2008.** 49: **1254–1267.**

Supplementary key words lipid • central nervous system • ATPase binding cassette transporter

The central nervous system (CNS) is the richest repository of cholesterol in the body, containing 25% of the body's total cholesterol content but only 2% of its total mass (1). Approximately 70–80% of this cholesterol is stably sequestered in myelin, leaving a relatively small proportion found within highly dynamic neuronal and glial membranes (1). Nearly all brain cholesterol is synthesized in situ; quantitative analyses show that essentially no cholesterol carried on peripheral lipoproteins enters the brain across the blood-brain barrier (BBB) (1). During early development and myelination, the brain has a high demand for cholesterol biosynthesis, and both neurons and glia actively synthesize cholesterol de novo. However, cholesterol biosynthesis is reduced to a low basal rate in adult neurons, which rely largely on cholesterol delivered from glial-derived HDL-like particles enriched in apolipoprotein E (apoE) to meet their lipid requirements. In the CNS, apoE coordinates the mobilization and redistribution of cholesterol and phospholipids during development or in response to injury, and facilitates the membrane re-

This study was supported by operating grants from the Alzheimer's Society of Canada (C.L.W.), the American Health Assistance Foundation (C.L.W.), and the Canadian Institutes of Health Research (C.L.W., B.C., J.P.). J.D. is supported by the University of British Columbia Arthur June Williams postdoctoral fellowship. B.C. is a Michael Smith Foundation for Health Research Senior Scholar. C.L.W. is a CIHR New Investigator.

Manuscript received 23 October 2007 and in revised form 22 January 2008 and in re-revised form 21 February 2007 and in re-re-revised form 25 February 2008.

Published, JLR Papers in Press, February 26, 2008.
DOI 10.1194/jlr.M700481-JLR200

Abbreviations: AD, Alzheimer's disease; apoE, apolipoprotein E; APP, amyloid precursor protein; BAC, bacterial artificial chromosome; BBB, blood-brain barrier; CHO, Chinese hamster ovary; CNS, central nervous system; CSF, cerebrospinal fluid; CTF, C-terminal fragment; HEK, human embryonic kidney; HMG-CoAR, HMG-CoA-reductase; LTP, long-term potentiation; LXR, liver X receptor; mAβ, murine Aβ; NGM, neuron growth media; QRT-PCR, quantitative reverse transcriptase PCR.

[1]To whom correspondence should be addressed.
e-mail: Cheryl@cmmt.ubc.ca

modelling that is associated with synaptic replacement, nerve terminal sprouting, and dendritic remodelling (2, 3). Because cells within the CNS cannot degrade the sterol ring, excess neuronal cholesterol is eliminated from the brain via cyp-46-mediated conversion of cholesterol to 24S-hydroxycholesterol, an oxysterol that can passively diffuse across the BBB into the peripheral circulation (4–6). Cyp46-deficient mice are impaired in cholesterol turnover and compensate by reducing net sterol synthesis (6, 7), demonstrating that the brain, like peripheral tissues, tightly regulates the balance of sterol synthesis and elimination by multiple modes of feedback control that converge upon HMG-CoA-reductase (HMG-CoAR), which catalyses the rate-limiting step in sterol biosynthesis.

Intriguingly, a low but continuous flux of sterol synthesis and export is required for normal learning and memory; mice lacking cyp46 have no demonstrable long-term potentiation (LTP) and are profoundly impaired in spatial memory tasks (7). LTP in brain slices prepared from cyp46-knockout mice is rescued by geranylgeraniol but not by cholesterol, indicating that the isoprenoid branch of the cholesterol biosynthetic pathway plays a crucial role in cognition (7). Together, these observations suggest that gene products that participate in maintaining sterol homeostasis in the CNS may have important roles for several brain functions, including myelination, neuronal repair, and cognition.

Several lines of evidence suggest that impaired brain cholesterol metabolism may also contribute to the pathogenesis of Alzheimer's disease (AD) (8). Allelic variation in apoE, the major cholesterol carrier in the CNS, is the best-established genetic risk factor for late-onset sporadic AD (9–11). Although the mechanisms by which apoE participates in AD pathogenesis remain a subject of considerable investigation, we and others have recently demonstrated that the lipidation status of apoE participates in the metabolism of Aβ peptides, which are the toxic products that accumulate as amyloid plaques in the brains of AD patients (12). In the brain, apoE is primarily lipidated by the cholesterol transporter ABCA1; mice deficient in ABCA1 have low levels of poorly lipidated apoE in brain tissues and in cerebrospinal fluid (CSF) (13, 14). Intriguingly, several groups including ours have shown that ABCA1-deficient animals have an increased amyloid load when crossed to mouse models of AD, suggesting that poorly lipidated apoE promotes amyloidogenesis in vivo (15–17). Conversely, increasing ABCA1 levels by 6-fold or greater increases apoE lipidation and virtually eliminates amyloid burden in the PDAPP model of AD (18). Although whether the lipidation status of apoE primarily affects Aβ deposition or influences Aβ clearance remains to be fully elucidated, existing studies identify ABCA1-mediated lipidation of apoE as a significant contributing factor to amyloid burden in vivo.

A second mechanism whereby cholesterol may contribute to the pathogenesis of AD is the generation of Aβ from amyloid precursor protein (APP), which is influenced by the concentration and distribution of cholesterol in cellular membranes (8, 19). APP is a type I transmembrane protein that is cleaved along two major proteolytic pathways (20). APP can be cleaved by β-secretase (encoded by BACE-1) to release a soluble N-terminal domain of APP into the extracellular space and leave a 99-amino-acid (C99) C-terminal fragment (CTF) attached to the plasma membrane (21). β-secretase activity is thought to occur primarily in lipid rafts, which are detergent-insoluble microdomains rich in cholesterol and sphingomyelin (22). C99 is further cleaved by γ-secretase (a complex composed of presenilin, nicastrin, aph1, and pen2) within the membrane to release the APP intracellular domain and liberate Aβ peptides, typically 40 or 42 amino acids in length (23). The first step in APP cleavage can also be mediated by α-secretase, which cleaves within the Aβ domain and thereby precludes the formation of Aβ species (20). Multiple proteins of the ADAM family are reported to possess α-secretase activity, and the activity of ADAM 10 is modulated by the fluidity of the membrane (24–26). Several studies have shown that conditions of high membrane cholesterol content promote Aβ generation by facilitating the interaction of APP and BACE-1 in lipid rafts (27–30). Conversely, depletion of membrane cholesterol by either pharmacological or biochemical means increases α-secretase activity and decreases Aβ production (22, 24, 31–34). These studies suggest that genes that control the levels or distribution of cellular cholesterol could influence Aβ generation by affecting the accessibility of APP to secretase components, or through direct effects on secretase activity.

ABCG1 is a member of the ATP binding cassette superfamily and part of a network of genes that regulate cellular lipid homeostasis (35). In cultured cells, ABCG1 promotes the efflux of cholesterol, phospholipid, sphingomyelin, and 7-ketocholesterol (36–40). These studies have led to a model whereby ABCA1 catalyses the initial transfer of lipids onto lipid-free apolipoproteins, including apoA-I or apoE, to form nascent discoidal particles, which are then fully lipidated in a second phase of efflux mediated by ABCG1 (41, 42). In vivo, however, the roles of ABCG1 are less well understood. Several studies have clearly demonstrated that neither overexpression nor deficiency of ABCG1 affects plasma lipid levels, although a recent investigation observed reduced nonesterified fatty acids in ABCG1-deficient mice fed a high-fat diet devoid of cholesterol (43–49). Several groups have shown that deficiency of ABCG1 leads to accumulation of neutral lipids in several peripheral tissues when animals are challenged with a high-fat diet containing cholesterol, supporting a role for ABCG1 in the regulation of tissue sterol homeostasis (43, 44, 47). ABCG1 is abundantly expressed in macrophages, yet despite several studies, consensus has not yet been reached as to whether ABCG1 is pro- or anti-atherogenic (45–48, 50, 51). ABCG1 is also highly expressed in brain (52–54), and cholesterol efflux from primary cerebellar glia has been reported to correlate better with ABCG1 than ABCA1 (55). Recently, ABCG1 has been shown to mediate intravesicular cholesterol transport of sterols in primary neurons and astrocytes, to influence SREBP-2 processing, and to affect SREBP-2-responsive genes in the CNS (54).

Two independent studies have shown that the cholesterol transporter ABCG1 influences APP processing in cultured cells, but reach opposite conclusions about the effect of ABCG1 on Aβ production. Tansley et al. (52) demonstrated that transient transfection of ABCG1 into human embryonic kidney (HEK) 293 cells expressing APP containing the Swedish mutation (APPSwe) increased Aβ40 and Aβ42 levels by approximately 30%. In contrast, Kim et al. (56) observed that Aβ production was suppressed by 64% in Chinese hamster ovary (CHO) cells coexpressing APP and ABCG1. These contrasting findings are reminiscent of early disparate reports on the potential role for ABCA1 in Aβ production in cellular models (57–59). Importantly, later studies subsequently demonstrated that ABCA1 has no detectable role in Aβ production in vivo (15–17, 60). Rather, ABCA1 influences amyloid burden through its effects on apoE lipidation, which is hypothesized to affect Aβ deposition or clearance. These studies highlight the importance of evaluating potential regulators of Aβ production in an appropriate in vivo setting.

Determining the in vivo role of ABCG1 in AD pathogenesis is particularly important given that synthetic liver X receptor (LXR) agonists such as T0901317 and GW3695 have been observed to reduce Aβ production, amyloid burden, and cerebral inflammation in AD mice (61–64), and ABCG1 is highly induced by LXR stimulation. Although these compounds also stimulate the expression of other genes in addition to ABCG1, clarification of which gene or genes mediate the beneficial effects of LXR agonists in AD possesses considerable therapeutic potential. We therefore determined whether selective ABCG1 overexpression affected neuropathological and cognitive phenotypes of the PDAPP mouse model of AD, and evaluated the role of ABCG1 deficiency in endogenous Aβ metabolism. Here we report that ABCG1 levels did not influence Aβ production or apoE levels in brain. Robust overexpression of ABCG1 in glia and neurons and a 6-fold increase in protein also did not affect measures of learning and memory under baseline conditions or exacerbate Aβ-related cognitive deficits. ABCG1 protein levels were, however, inversely correlated with the levels of cholesterol biosynthetic intermediates and the cholesterol catabolite 24S-hydroxycholesterol in brain, and ABCG1 levels were positively correlated with SREBP-2 and HMG-CoAR mRNA levels. These findings provide further support that ABCG1 participates in the regulation of brain sterol biosynthesis in vivo.

MATERIALS AND METHODS

Animals and tissue preparation

ABCG1-bacterial artificial chromosome (BAC)-transgenic (Tg) mice were generated by oocyte injection. Briefly, the 141 kb BAC CTD-2010I3 that contains the entire human ABCG1 genomic sequence plus 30.6 kb of 5′ and 13.1 kb of 3′ flanking sequences including LXR regulatory signals was microinjected into F1 C57Bl/6/CBA oocytes and backcrossed onto a pure C57Bl/6 genetic background for at least 10 generations. ABCG1-deficient mice (Deltagen, San Mateo, CA) were backcrossed to C56Bl/6 mice for at least 9 generations before use. The targeting vector used to generate these mice contained 7 kb of 5′ and 1.4 kb of 3′ murine genomic DNA flanking a 7 kb internal ribosome entry site-LacZ-Neo-pA cassette, and homologous recombination results in the deletion of seven amino acids (GPSGAGK) within the Walker A motif in exon 3 of the murine *abcg1* gene. PDAPP mice overexpress human APP_{751} with the familial AD mutation at position 717 (APP^{V717F}) under the control of the neuronal-specific platelet-derived growth factor promoter, and are on a C57Bl/6, Smith-Webster and DBA mixed genetic background (65). PDAPP animals homozygous for the APP transgene were crossed to ABCG1-BAC-Tg hemizygotes to generate experimental cohorts (N = 20–24). To control for the possibility that gender may influence the baseline rate of amyloid deposition in PDAAP mice, male mice were used for all studies involving Aβ or amyloid quantitation. All animals were maintained on a standard chow diet [PMI LabDiet 5010 (St. Louis, MO), containing 24% protein, 5.1% fat, and 0.03% cholesterol]. To collect tissue samples or CSF, mice were first anesthetized by intraperitoneal administration of 600 mg/kg Avertin (Sigma-Aldrich, St. Louis, MO) or an intramuscular administration of a mixture of 20 mg/kg xylazine (Bayer, Pittsburgh, PA) and 150 mg/kg ketamine (Bimeda-MTC, Cambridge, Ontario, Canada), and CSF was isolated from the cisterna magna as previously described (66). Animals were then perfused for 7 min with PBS containing 2,500 U/l heparin, and brains were collected, dissected as required, and either snap frozen at −80°C or postfixed for thioflavin-S histology as previously described (15). All procedures involving experimental animals were approved by the Canadian Council of Animal Care and the University of British Columbia Committee on Animal Care.

Primary culture and LXR treatment

Primary neurons were prepared from E16 or E17 murine embryos. Embryonic brains were removed and placed in cold HBSS containing 6 g/l glucose and 50 mM HEPES. Hippocampi/cortices were isolated, stripped of meninges, and minced with forceps. Minced tissue was incubated for 3–10 min in 0.05% trypsin at 37°C until addition of 2 vols of Stop Media [Neurobasal media; 10% FBS, 0.5 mM L-glutamine, B27 supplement, 1% penicillin/streptomycin (Invitrogen, Carlsbad, CA)] and then triturated gently through sterile 5 ml pipettes. Homogenates were centrifuged for 3 min at 1,000 *g*, resuspended in neuron growth media (NGM) (Neurobasal media; 0.5 mM L-glutamine, B27 supplement, 1% penicillin/streptomycin), and gently triturated through fire-polished glass pipettes to create a single cell suspension. Crude cellular debris was allowed to settle for 1 min before transferring cells to a fresh tube. Neurons were seeded at a density of one mouse per 24-well plate prepared by overnight coating with 0.1 mg/ml poly-D-lysine (Sigma-Aldrich). Neurons were maintained in NGM that was 1/2 changed with fresh NGM every 4 days for a total of 14 days in vitro prior to treatment with DMSO (vehicle) or DMSO with 1 μM TO901317 for 24 h.

Primary astrocytes were obtained from postnatal day 1–2 pups. Brains were removed and placed in cold HBSS adjusted to 6 g/l glucose and 10 mM HEPES buffer. Meninges were removed, cortices and hippocampi were isolated and minced and then homogenized by shearing through a 5 ml sterile tissue culture pipette. Triturated brain samples were centrifuged at 1,000 *g* for 5 min. The supernatant was discarded, and homogenized tissue samples were resuspended in 1 ml of growth media (Invitrogen; DMEM-F12 containing 10% FBS, 2 mM L-glutamine, 1% penicillin/streptomycin). Each cell suspension from an individual pup was seeded in one T75 tissue culture flask. Media was changed

every 3–5 days until cells were fully confluent at approximately 12–14 days prior to treatment with or without 1 μM TO901317.

Protein extraction and Western blotting

For analysis of ABCG1 protein expression in tissues, total membranes were purified as described (67). Briefly, to prepare crude membrane fractions from frozen tissue, tissues were homogenized in 5 vols of lysis buffer [50 mM mannitol, 2 mM EDTA, 50 mM Tris HCl, pH 7.6, and complete protease inhibitor (Roche, Indianapolis, IN)], and centrifuged at 500 *g* to pellet nuclei and debris. Supernatant (400–450 μl) was layered onto 600 μl of fractionation buffer (300 mM mannitol, 2 mM EDTA, 50 mM Tris HCl, pH 7.6) and centrifuged at 100,000 *g* for 45 min to pellet total membranes. Membranes were resuspended in 150–200 μl of lysis buffer. SDS was added to a final concentration of 1% prior to Tris-glycine SDS-PAGE and immunoblotting with antibodies against ABCG1 (Novus, Littleton, CO) and Na/K-ATPase (Novus) as an internal loading control. For analyses of APP CTFs and apoE, tissues were lysed in lysis buffer consisting of 20 mM Tris-HCl, pH 7.4, 5 mM EDTA, 50 mM NaCl, 10 mM Na pyrophosphate, 50 mM NaF, 1% NP40, and complete protease inhibitor. Lysates were sonicated for 20 s and centrifuged for 5 min at 11,000 *g*, and the supernatants were collected. Thirty micrograms of protein were loaded per lane on 4%-10%-17% step gradient Tris-tricine gels with an anode buffer consisting of 0.2 M Tris-HCl, pH 8.9, and a cathode buffer consisting of 0.1 M Tris-HCl, pH 8.4, 0.1 M tricine, and 0.1% SDS. Following electrophoresis, proteins were transferred to nitrocellulose membranes and probed with anti-APP C-terminal (Sigma-Aldrich) antibodies to detect CTFα or CTFβ. To detect total brain ABCA1 and apoE levels, hemi-brains were homogenized in lysis buffer, sonicated for 20 s, and centrifuged at 11,000 *g* to remove debris. Cleared lysates were run separated by Tris-glycine SDS-PAGE, and membranes were probed with anti-ABCA1 (68) and anti-apoE M-20 (Santa Cruz Biotech; Santa Cruz, CA). ApoE in CSF or plasma was also detected by M-20 immunoblot. Blots were developed using enhanced chemiluminescence (Amersham, Pittsburgh, PA) according to the manufacturer's recommendations, and quantitated using densitometry. Photographic film was scanned into TIFF format at 600 dpi resolution, and pixel counts were determined using ImageJ (National Institutes of Health, Bethesda, MD) software.

RNA extraction and quantitative RT-PCR

RNA was extracted using Trizol (Invitrogen,). Samples were treated with DNaseI prior to cDNA synthesis. cDNA was generated using oligo-dT primers and Taqman reverse transcription reagents (Applied Biosystems, Foster City, CA). Primers were designed using PrimerExpress software (Applied Biosystems) and spanned exons 22–23 of human ABCG1. Sequences are: Human ABCG1 forward (5′ ACACCATCCCCACGTACCTA 3′) and reverse (5′ GATGACCCCTTCGAACCCA 3′), murine ABCG1 forward (5′ CAACGTGGATGAGGTTGAGA 3′) and reverse (5′ CTGGGCCTCTGTGAAGTTGT 3′), SREBP-2 forward (5′ GCGTTCTGGAGACCATGGA 3′) and reverse (5′ ACAAAGTTGCCTGAAAACAAATCA 3′), HMG-CoAR forward (5′ CTTGTGGAATGCCTTGTGATTG 3′) and reverse (5′ AGCCGAAGCAGCACAATGT 3′), and murine β-actin forward (5′ ACGGCCAGGTCATCACTATTG 3′) and reverse (5′ CAAGAAGGAAGGCTGGAAAAG 3′). Quantitative reverse transcriptase PCR (QRT-PCR) was done with Sybr green reagents (Applied Biosystems) on an ABI 7000. Cycling conditions were 50°C for 2 min, 95°C for 10 min, then 40 cycles at 95°C for 15 s and 60°C for 1 min, followed by dissociation at 95°C for 15 s, 60°C for 20 s, and 95°C for 15 s Each sample was assayed at least in triplicate, normalized to β-actin ,and analyzed with 7000 system SDS software v1.2 (Applied Biosystems) using the relative standard curve method.

Analysis of Aβ levels

For studies analyzing ABCG1 in the presence of the PDAPP transgene, hippocampal brain tissues were subjected to a serial extraction with PBS, 100 mM carbonate, and 5 M guanidine, and the resulting solubilized pools of Aβ were measured by sandwich ELISA as described (69). The antibody combinations employed in the ELISA were specific for full-length human Aβ1-40 (2G3 capture and biotinylated 3D6 report) or Aβ1-42 (21F12 capture and biotinylated 3D6 report). The human Aβ levels were expressed relative to total protein. For studies analyzing endogenous murine Aβ (mAβ), hemi-brains were solubilized directly in 5 M guanidine, and diluted extracts were quantified by ELISA. To measure rodent Aβ, C-terminal antibodies 2G3 (Aβ40 specific) and 21F12 (Aβ42 specific) were used as capture, and biotinylated m266 (central domain specific) was used as the reporting antibody. mAβ levels were expressed relative to total protein. Total cellular protein was determined by BCA protein assay (BioRad, Hercules, CA).

Cholesterol efflux

Cholesterol efflux from primary glia was performed as described previously (13). Briefly, glia were seeded into 24-well dishes at 200,000 cells/well, and loaded with DMEM containing 1% FBS, 40 μg/ml acetylated low-density lipoprotein, and 2 mCi H^3-labeled cholesterol for 24 h. Cholesterol-laden glia were then washed two times with PBS and equilibrated in serum-free DMEM for 2 h prior to the addition of efflux media consisting of DMEM supplemented with 0.2% BSA and either 15 μg/ml human recombinant apoA-I (Calbiochem, San Diego, CA),

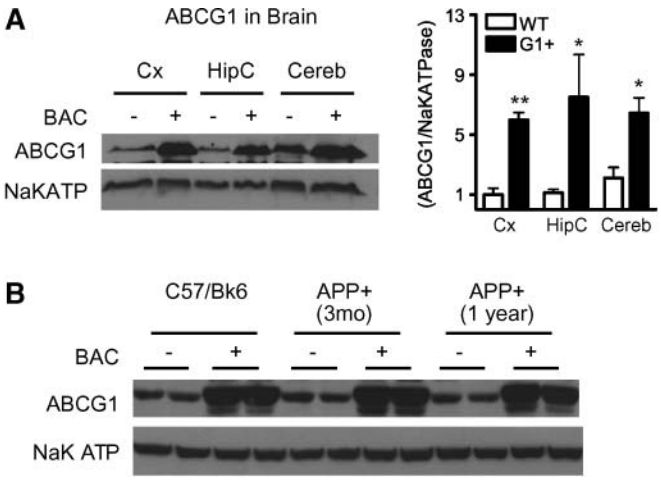

Fig. 1. ABCG1-bacterial artificial chromosome-transgenic (ABCG1-BAC-Tg) mice overexpress ABCG1 in cortex, hippocampus, and cerebellum. To confirm overexpression of ABCG1 protein, crude membrane fractions were extracted from dissected brain regions and were subjected to Western blot. Blots were probed by polyclonal antibodies recognizing human and mABCG1 or Na/K-ATPase as a loading control. A: ABCG1 protein levels are increased 6-fold in cortex (Cx) and hippocampus (HipC) and 3-fold in cerebellum (Cereb) of ABCG1-BAC-Tg mice relative to baseline levels in the equivalent region from wild-type (WT) controls. Western blots were summarized by densitometry and normalized to wild-type cortical levels (N = 3). Error bars indicate ± SEM. * $P < 0.05$, ** $P < 0.001$. B: ABCG1 protein levels are unaffected by the presence in the human APP transgene alone at 3 months of age, or by subsequent amyloid deposition at one year of age (N = 2). APP, amyloid precursor protein.

15 μg/ml human apoE3 (Calbiochem), or 25 μg/ml human HDL2/3. After 4 h, efflux media was collected and cells were lysed in 0.1% SDS, 0.1% NaOH, and radioactivity was determined by scintillation counting. Efflux is defined as media counts/(media counts + cell counts).

Behavioral analysis

Animals were individually housed for 2 weeks prior to behavioral testing, and were maintained on a 12 h dark/12 h light cycle. All testing was performed during the dark cycle, when the animals are naturally active. The animals were approximately 12 months old (±0.45) at the time of testing. To avoid extra stressors that could affect performance, cages were changed once a week following a testing session and the mice were handled only by a single experimenter. Learning and memory were assessed using Morris water maze tasks in a circular white pool (100 cm diameter, 54 cm height) filled with 22°C water to a height of 36 cm. Distinct geometric shapes were attached to the walls of the pool on three sides, and the experimenter and computer system were hidden behind a dividing wall. A circular platform (14 cm diameter, 35 cm height) was submerged 1 cm below the surface. For each trial, a mouse was released into the pool at one of three positions and allowed to search for the platform. Each trial lasted a maximum of 60 s, after which the mouse was manually guided to the platform and allowed to remain on it for 10 s. All trials were tracked using an overhead digital camera and ANY-maze video tracking system (Stoelting, ,Wool Dale, IL). The reference memory task was used to assess learning and long-term memory for a fixed platform location. Mice were trained for four trials per day, for a total of 5 days. Twenty-four hours after the last training session, a probe trial was administered in which the platform was removed and the mouse was allowed to swim freely for 60 s, and the amount of time spent in the quadrant of the pool that had previously contained the platform was measured. The following day, training sessions resumed with the platform relocated to the opposite quadrant. Mice were trained on this new location for 3 more days. Twenty-four hours following the last training session a second probe trial was administered. Both groups of mice received a total of 36 training trials and two probe trials each during the reference memory task. The spatial working memory task was used to assess deficits in working memory. The pool was set up as described above, except that the platform location was changed to a new location on a daily basis. Mice were assessed with two trials per day, for 4 days. A decrease in latency to the platform on the second trial of the day was an indicator of functional working memory. Mice were screened for inappropriate behaviors in the water maze, such as spinning, thigmotaxis around the perimeter of the pool, and floating. An equal proportion (approximately 5%) of mice from each group displayed such behaviors and were removed from the study.

Quantitative analysis of sterols, intermediates, and metabolites

Lipids were extracted from brain tissue by a modified Folch procedure as described (70, 71). Dried tissue samples were submerged in chloroform-methanol (2:1) overnight. Solvent volume was adjusted to 20× the dry weight, and 0.25× vols of 0.9%

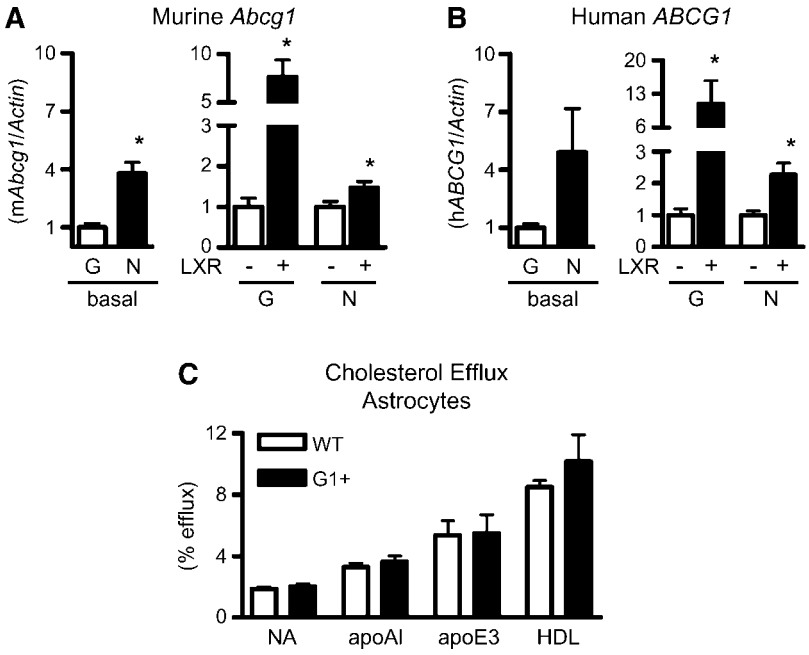

Fig. 2. Cell-specific expression of murine *Abcg1* and human *ABCG1* in primary cells. To measure *Abcg1* expression in primary cells, neurons (N) cultured from E16 embryos and mixed glia (G) prepared from postnatal pups were seeded in 12-well plates and treated with either vehicle (−), or 1 μM liver X receptor (LXR) agonist TO901317 (+) for 24 h. mRNA was quantified by quantitative reverse transcriptase (QRT)-PCR using intron-spanning primers specific to human or murine *Abcg1* isoforms and was normalized to *Actin* as a control. To compare basal expression between astrocytes and neurons, ABCG1 mRNA levels were normalized to those in untreated astrocytes. To evaluate LXR responsiveness in each cell type, data were expressed relative to untreated controls. A: Murine *Abcg1* expression. B: Human *ABCG1* expression. * $P < 0.05$. C: Excess ABCG1 does not increase cholesterol efflux from Ac-LDL-treated primary glia to human apolipoprotein A-I (apoA-I) (15 μg/ml). apoE3 (15 μg/ml), or HDL2/3 (25 μg/ml). Data represent the means and standard deviation from N = 3 independent samples from wild-type (white bars) and ABCG1-BAC-Tg (black bars).

NaCl was added, mixed vigorously for 1 min, and equilibrated by shaking for 2 h at room temperature. Samples were centrifuged at 2,000 rpm for 5 min to separate phases. The upper aqueous phase was removed, and lipids were dried under N_2. Sterol levels were determined after derivatization to the corresponding trimethylsilyl-ethers by gas chromatography-flame ionization detection and GC-MS.

Statistical analysis

Data were analyzed by Student's *t*-test unless specifically stated in the figure legend or a one-way ANOVA with Newman-Keuls post test performed by GraphPad Prism (version 4.0) software. All in vivo data were conducted with the rater blinded to genotype.

RESULTS

ABCG1 protein is overexpressed by at least 6-fold in brain regions

ABCG1-BAC-Tg mice express human ABCG1 and exhibit a 2- to 4-fold elevation of ABCG1 protein in peripheral tissues, including liver, spleen, lung, and peritoneal macrophages (Burgess et al., under revision). Furthermore, human ABCG1 functionally compensates for loss of endogenous murine ABCG1 and completely prevents lipid accumulation in the lungs of mice challenged with a high-fat, high-cholesterol diet (Burgess et al., under revision), conclusively proving that the human ABCG1 transgene is functional in vivo. To confirm that these ABCG1-BAC-Tg mice also exhibit the expected increase in ABCG1 protein levels in brain, Western blots were prepared from crude membrane fractions of cortex, hippocampus, and cerebellum. Compared with the levels in wild-type cortex, ABCG1 protein levels in ABCG1-BAC-Tg mice were increased by approximately 6-fold ($P < 0.001$, N = 3) in cortex, 8-fold ($P < 0.05$, N = 3) in hippocampus, and 6-fold ($P < 0.05$, N = 3) in cerebellum (**Fig. 1A**). These data demonstrate that the ABCG1-BAC is robustly expressed in brain under baseline conditions.

Because these ABCG1-BAC-Tg mice would be used to study the effect of excess ABCG1 on Aβ metabolism, we further verified that ABCG1 protein levels remained elevated in hippocampus (Fig. 1B) and cortex (not shown) after crossing to PDAPP mice (ABCG1/PDAPP mice). This test is important because we have previously shown that expression of a related cholesterol transporter, ABCA1, was altered in APP-Tg mice (72). Unlike ABCA1, however, expression of endogenous and transgenic ABCG1 is unaffected by the presence of Aβ or amyloid in ABCG1/PDAPP brain at either 3 months or 1 year of age (Fig. 1B).

ABCG1 expression is appropriately regulated in neurons and astrocytes but does not promote cholesterol efflux

To confirm appropriate regulation of ABCG1 in specific cell types, murine and human ABCG1 mRNA was isolated from neurons and astrocytes, before and after LXR stimulation. Neurons were harvested from E16 embryos and cultured for 14 days. Astrocytes were cultured from postnatal day 1–2 pups for approximately 2 weeks. Cells were treated with 1 μM TO901317 for 24 h prior to QRT-PCR analysis of ABCG1 mRNA levels. Murine *Abcg1* mRNA levels were approximately 4-fold higher in untreated neurons compared with astrocytes (**Fig. 2A**). After LXR stimulation, *Abcg1* mRNA levels rose approximately 7-fold in astrocytes but approximately 1.5-fold in neurons. Human ABCG1 also showed similar responses, with 5-fold higher basal expression in neurons compared with astrocytes, and a more prominent response to LXR induction in astrocytes (11-fold) compared with neurons (2.5-fold) relative to untreated cells (Fig. 2B). These data confirm previous reports of ABCG1 expression in neurons and astrocytes and demonstrate LXR responsiveness in both cell types (55, 56). Nevertheless, the increased ABCG1 levels in untreated cells were not associated with elevated cho-

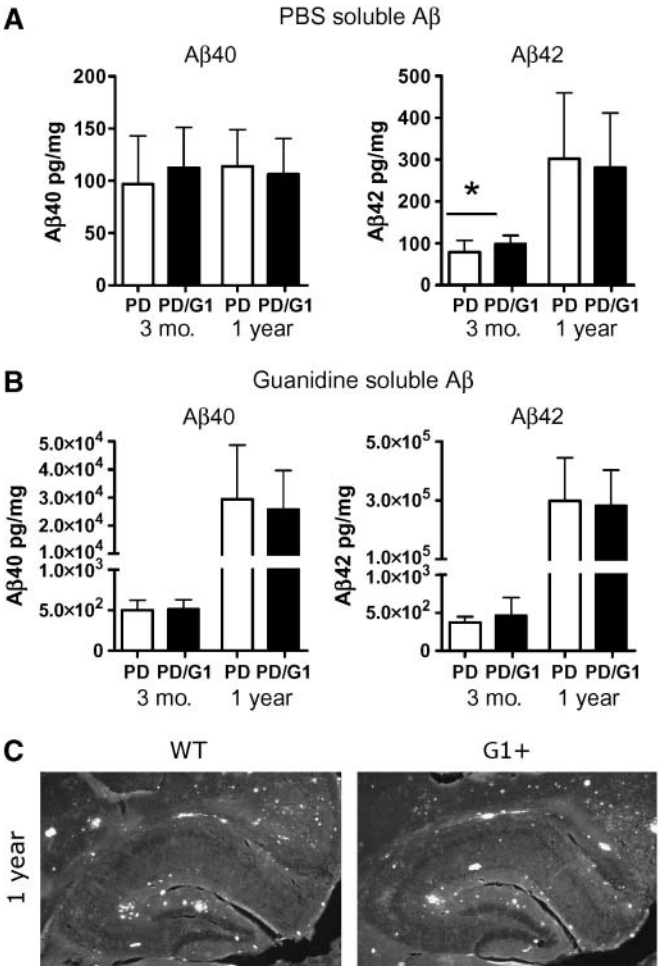

Fig. 3. ABCG1 overexpression is not a major regulator of PBS- or guanidine-soluble Aβ levels in young or aged PDAPP hippocampi. Hippocampi from PDAPP mice (PD) or PDAPP/ABCG1-BAC-Tg mice (PD/G1) aged 3 months or 1 year were serially extracted in PBS and guanidine hydrochloride, respectively, and analyzed by ELISA for total Aβ or Aβ42. A: ABCG1 overexpression increased PBS-soluble levels of Aβ42 in 3-month-old animals ($P < 0.05$, N = 18) but did not significantly affect Aβ40 or Aβ42 in aged animals (N = 24). B: ABCG1 overexpression did not affect guanidine-extractable levels of Aβ40 or Aβ42 ($P > 0.05$; N = 18). C: Representative sections stained with thioflavin-S show that levels and distribution of amyloid are indistinguishable between 1-year-old ABCG1/PDAPP brains.

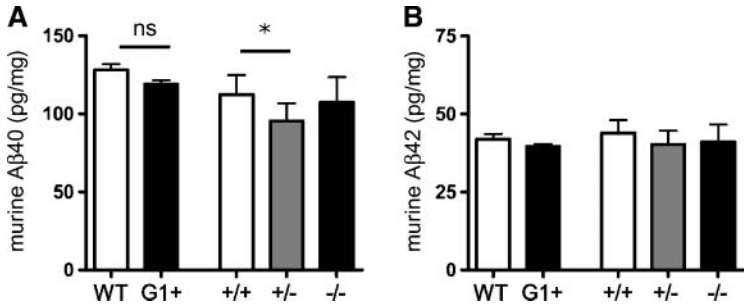

Fig. 4. Hemizygosity of ABCG1, but not complete deficiency or overexpression, is associated with decreased murine Aβ40 (MAβ40). To determine whether ABCG1 influences mAβ metabolism, whole brains lacking human APP were homogenized in guanidine and subjected to ELISA. Aβ measurements were normalized to total protein content. A: Aβ40 levels were significantly reduced in *Abcg1*$^{+/-}$ compared with $^{+/+}$ animals (* $P < 0.05$, N = 7), but no significant difference was observed between either ABCG1-BAC-Tg mice (G1+) and wild-type (WT) animals, or between *Abcg1*$^{-/-}$ and *Abcg1*$^{+/+}$ controls (N = 7). B: Aβ42 levels were not significantly affected by ABCG1 overexpression or deficiency when compared with the appropriate littermate controls. Data represent mean and standard deviation of a minimum of seven independent samples. Wild-type and ABCG1-Tg groups were compared by Students *t*-test, and *Abcg1*-deficient animals and controls were compared using a one-way ANOVA.

lesterol efflux from acetylated-LDL-treated primary glia to any lipid acceptor tested, including delipidated apoA-I, apoE3, fully lipidated HDL2/3, or nascent apoE-containing particles from astrocyte-conditioned media (Fig. 2C).

ABCG1 levels do not influence Aβ levels or amyloid burden in vivo

We previously observed that expression of ABCG1 in HEK cells stably expressing APP with the Swedish mutation (HEK-APPswe) resulted in increased Aβ production, whereas Kim et al. (52, 56) reported the opposite finding of reduced Aβ production from CHO-APP cells. To determine whether ABCG1 overexpression affects Aβ levels in vivo, ABCG1-BAC-Tg mice were crossed to PDAPP animals, and hippocampal Aβ measurements were taken at 3 months and 1 year of age to encompass incipient and early stages of amyloid deposition. Brain tissues were extracted first by PBS to remove soluble Aβ species, then with high-pH carbonate to remove the peripherally associated membrane fraction, and finally with guanidine hydrochloride to extract insoluble Aβ, including fibrillar aggregates. PBS-soluble Aβ40 levels were not significantly affected by ABCG1 overexpression at 3 months ($P = 0.30$, N = 18) or 1 year of age ($P = 0.71$, N = 24) (**Fig. 3A**). Although PBS-soluble Aβ42 levels in hippocampus of 3-month-old ABCG1-BAC-Tg mice showed a statistically significant increase of 1.2-fold ($P < 0.05$, N = 18) compared with littermate controls (Fig. 3A), excess ABCG1 was not associated with significant changes in PBS-soluble Aβ42 ($P = 0.90$, N = 24) at 1 year. No significant alterations were observed in the carbonate extractions for either age (data not shown). Furthermore, neither guanidine-soluble Aβ42 nor Aβ40 levels were affected by ABCG1 expression at either age (Fig. 3B). These data show that although excess ABCG1 was associated with a subtle increase in soluble Aβ42 levels in early disease, there was no correlation between ABCG1 level and guanidine-soluble Aβ species in aged mice. Amyloid levels and distribution were also indistinguishable between ABCG1 wild-type and overexpressing mice as determined by thioflavin-S staining (Fig. 3C).

To determine whether ABCG1 gene dose affected endogenous Aβ levels, we then measured mAβ in animals lacking the human APP transgene. Guanidine brain lysates from wild-type, ABCG1-BAC-Tg, and ABCG1$^{-/-}$ mice in the absence of any Aβ or amyloid deposits were therefore prepared. mAβ40 and Aβ42 levels were indistinguishable in ABCG1-BAC-Tg mice compared with littermate controls

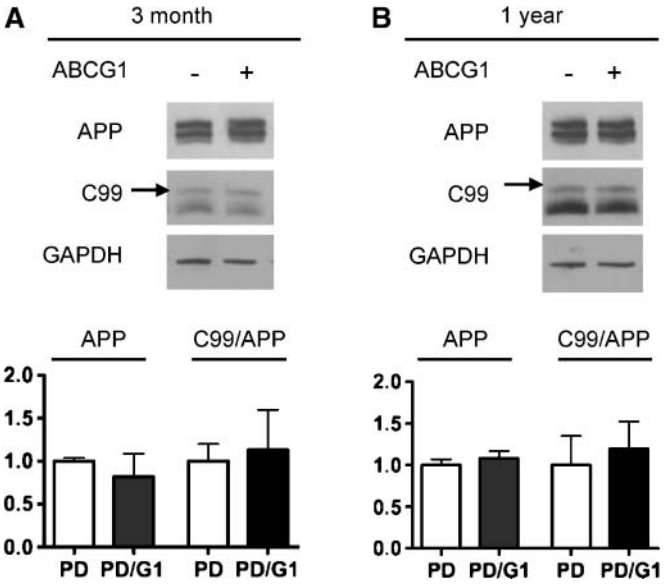

Fig. 5. C99 and total APP levels are not affected by ABCG1 overexpression. APP and C99 levels in hippocampus of 3-month-old (A) or 1-year-old (B) PDAPP mice (PD) or PDAPP/ABCG1-BAC-Tg mice (PD/G1) were measured by Western blot. Membranes were probed with antibodies specific to the C terminus of human APP, and the results were quantified by densitometry from duplicate gels for comparison. C99 levels are expressed as a ratio of total APP. Data represent mean and standard deviation of N = 5 samples.

(**Fig. 4A**). Aβ42 levels were also unchanged in animals lacking one or both copies of ABCG1 (Fig. 4B). Intriguingly, mAβ40 levels in ABCG1 hemizygote ($^{+/-}$) animals were significantly reduced by 15% relative to wild-type littermates ($P < 0.01$, N = 7). However, this effect was not observed in animals fully deficient ($^{-/-}$) for ABCG1 ($P = 0.51$, N = 7), suggesting the possibility that compensatory gene expression in the complete absence of ABCG1 may restore steady-state Aβ levels. Taken together with the measurement of human Aβ species, neither increases nor decreases in ABCG1 gene dose resulted in consistent or robust effects on Aβ40 or Aβ42 levels in vivo.

Total APP and C99 levels are unaffected by ABCG1 overexpression

Steady-state Aβ levels are a function of Aβ production and clearance. We previously showed that ABCG1 overexpression increased β-secretase cleavage of APP in HEK-APP cells (52), supporting a role for ABCG1 in Aβ generation. However, as a cholesterol transporter, ABCG1 may also contribute to apoE-mediated lipid homeostasis (48, 73), which in turn may contribute to Aβ clearance mechanisms. The lack of significant changes in steady-state Aβ levels in ABCG1/PDAPP mice could therefore be because ABCG1 has no effect on Aβ production in vivo, or could be due to a balanced increase in Aβ production and clearance that results in zero net change. To distinguish between these possibilities, Western blots were used to determine whether C99 levels were increased in the brains of ABCG1/PDAPP mice at 3 months and at 1 year of age as a direct measure of APP cleavage in vivo. Compared with littermate controls, ABCG1 overexpression did not significantly affect total APP or C99/APP levels at either age in hippocampus (**Fig. 5A, B**) or cortex (data not shown). The inability of excess ABCG1 to increase C99 levels strongly argues against a role for ABCG1 in APP processing in vivo.

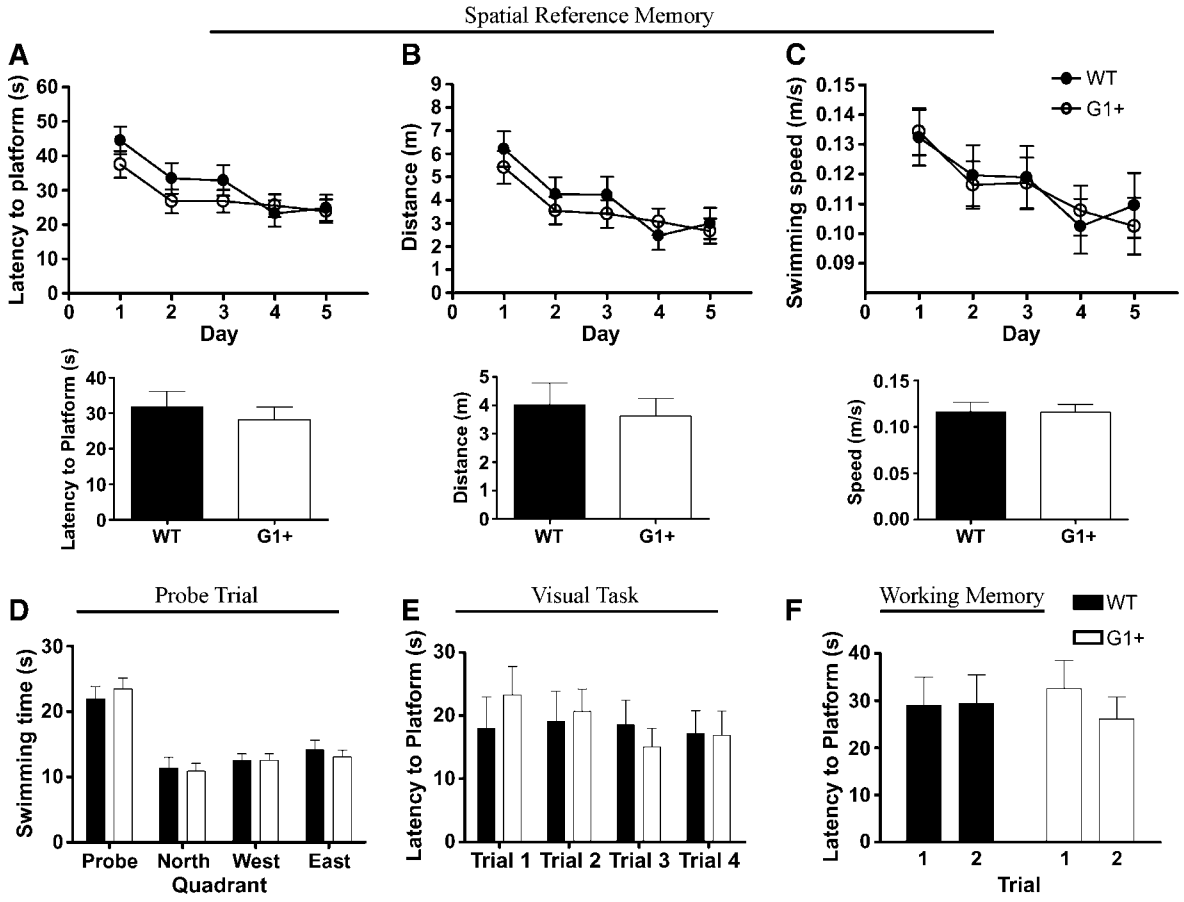

Fig. 6. Water maze performance of PDAPP BAC− or BAC+ mice. A–D: Results from spatial reference memory water maze task. Each point represents an average of four daily trials during the training period. Bars indicate the mean and standard deviations of performance for each measure over 5 days of training for wild-type (WT; filled symbols) and ABCG1-BAC-Tg (G1+; open symbols) groups, N = 23. A: Latency to platform. No significant difference was observed between the groups in the time taken to find the hidden platform. B: Swim distance. Both groups swam similar distances over the training period. C: Swim speed. Both groups of mice displayed similar mean swimming speed in the water maze pool. D: Probe trial results. Both groups showed similar preference for the probe quadrant, which contained the platform on training trials. Both groups displayed evidence of spatial memory, but there were no significant differences between groups. E: Visual test. No significant group differences were observed for the time it took mice to locate a visibly conspicuous escape platform. F: Spatial working memory water maze task. There was no significant difference in performance between the two groups, although the ABCG1-BAC-Tg group displayed a greater difference in latency to the platform between the two trials.

Overexpression of ABCG1 does not influence cognitive performance of PDAPP mice

Deficits in spatial learning that worsen with age have previously been characterized in the PDAPP mouse model (74). To determine if excess ABCG1 affected the learning and memory of PDAPP mice, we evaluated Morris water maze performance of 12-month-old ABCG1/PDAPP compared with PDAPP animals. Preliminary behavioral tests found that excess ABCG1 did not adversely affect anxiety, locomotion, or vision (data not shown). On the spatial reference memory task (fixed location/hidden platform), no significant differences were found in the latency to the platform (**Fig. 6A**), swim path length (Fig. 6B), or swim speed (Fig. 6C) between the two groups. In the probe trial, both groups of mice displayed an equally strong preference for the quadrant that contained the platform during training trials, showing evidence of equivalent spatial memory for the original platform location (Fig. 6D). Additionally, excess ABCG1 did not influence the ability to detect a visible platform (Fig. 6E). On the spatial working memory task (submerged platform moved to a new location on a daily basis), no significant difference in performance between the two groups were noted on either of two trials conducted over the 4-day duration of this task (Fig. 6F).

ABCA1 and apoE levels are unaffected by ABCG1 gene dose

ApoE is central to the progression of AD neuropathology, particularly with respect to roles in the deposition or clearance of Aβ (69, 75, 76). ABCA1-mediated lipidation of apoE is a key determinant of amyloid burden in animal models of AD (15–17, 77). ABCG1 has been reported to facilitate apoE secretion from peripheral macrophages, and plasma apoE levels have been reported to be elevated in ABCG1$^{-/-}$ mice (48, 78) and to affect ABCA1 levels in macrophages (38). To determine whether ABCG1 overexpression or deficiency affected ABCA1 or apoE metabolism in the CNS, ABCA1 and apoE levels in brain of ABCG1-BAC-Tg and ABCG1-deficient mice were measured by Western blot (**Fig. 7A**). Neither ABCA1 nor apoE levels were affected by gain or loss of ABCG1, suggesting that ABCG1 is not a major determinant of apolipoprotein metabolism in brain. We also observed no change in plasma apoE levels in either ABCG1-BAC-Tg or ABCG1-deficient mice compared with wild-type littermates (Fig. 7B).

ABCG1 affects the cholesterol biosynthetic pathway in brain

Altered ABCG1 gene dose has been reported to impact cholesterol metabolism in peripheral tissues (43) (Burgess et al., under revision) and to influence SREBP-2 processing and SREBP-2-regulated genes in the CNS (54). To determine whether ABCG1 affects brain cholesterol homeostasis in vivo, the level of cholesterol, cholesterol biosynthetic intermediates, and cholesterol metabolites were measured by GC-MS (54, 79). Notably, we observed that the levels of the cholesterol intermediates lathosterol, lanosterol, and desmosterol were each significantly reduced in ABCG1-BAC-Tg mice compared with wild-type littermates. Specifically, lathosterol was reduced by 21% ($P < 0.01$, N = 8), lanosterol was reduced by 14% ($P < 0.01$, N = 8), and desmosterol was reduced by 27% ($P < 0.01$, N = 8) (**Fig. 8**). Correspondingly, ABCG1-deficient mice displayed complementary increases in these cholesterol intermediates in a gene dose-responsive manner ($P < 0.001$, N = 8) (Fig. 8). Although total cholesterol levels were unchanged by ABCG1 overexpression or deficiency, the levels of cholesterol catabolite 24S-hydroxycholesterol were significantly reduced by 15% ($P < 0.001$, N = 8) in ABCG1-BAC-Tg brain compared with controls and conversely increased by 20% ($P < 0.0001$, N = 8) in ABCG1-deficient mice. The levels of dietary-derived phytosterols were indistinguishable between experimental animals and controls (data not shown), demonstrating that the integrity of the BBB was not affected by ABCG1 level. Finally, no difference in peripherally derived oxysterol 27-hydroxycholesterol levels were observed between groups (data not shown), indicating that import of this oxysterol into the brain is unaffected by ABCG1 level.

Intriguingly, analysis of SREBP-2 and HMG-CoAR mRNA levels in brain tissue from ABCG1-BAC-Tg mice showed significantly elevated HMG-CoAR mRNA and a clear trend toward increased SREBP-2 mRNA levels in vivo compared

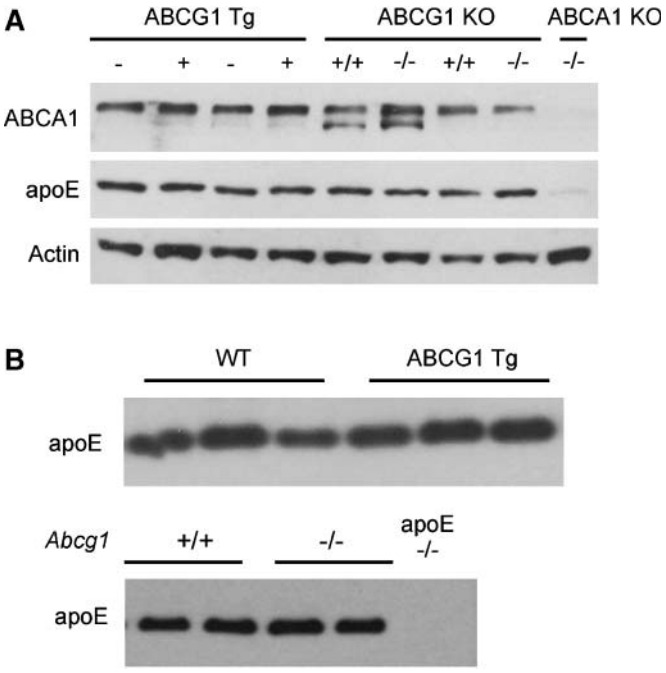

Fig. 7. ABCG1 does not change ABCA1 or apoE levels in brain or plasma. ABCA1 and apoE levels were determined by Western blot from either plasma or whole-brain lysates of experimental animals. Tissue blots are normalized to actin levels to control for protein loading. A: Brain lysates from ABCG1-BAC-Tg (+) and nontransgenic littermates (−), ABCG1-deficient ($^{-/-}$) and wild-type littermates ($^{+/+}$), and ABCA1-deficient animals show no difference in either ABCA1 or apoE levels. B: Plasma levels of apoE are unaffected by gain or loss of ABCG1. Equal volumes of plasma from wild-type ($^{+/+}$, WT), ABCG1-Tg, ABCG1-deficient ($^{-/-}$), and apoE-deficient ($^{-/-}$) mice were analyzed.

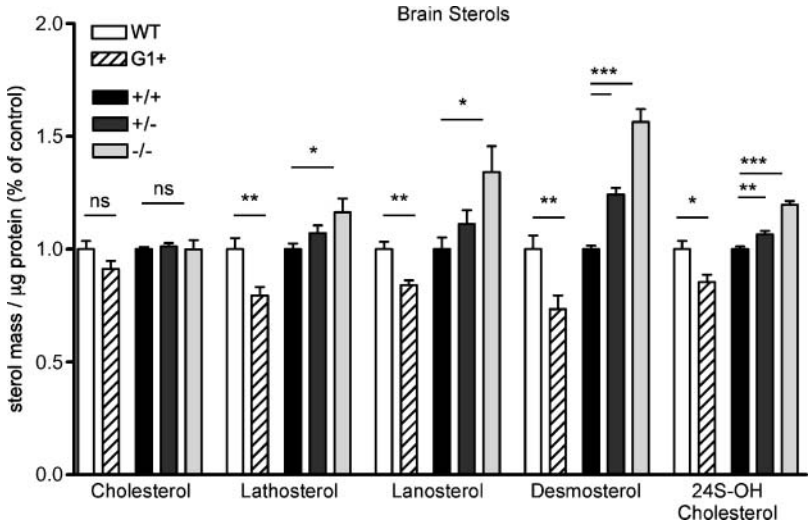

Fig. 8. Cholesterol precursor and metabolite levels in brain are inversely related to ABCG1 gene dose. Sterol levels were determined by GC-MS analysis of chloroform-methanol total lipid extracts prepared from whole brain of adult wild-type (WT) and ABCG1-BAC-Tg (G1+) mice, as well as wild-type ($^{+/+}$), hemizogous ($^{+/-}$), and homozygous ($^{-/-}$) ABCG1 animals. Sterol masses were normalized to those in littermate wild-type controls for comparison. Data represent means and standard deviation of N = 7 mice. Wild-type and ABCG1-Tg groups were compared by Student's *t*-test, and *Abcg1*-deficient animals and controls were compared using a one-way ANOVA. * $P < 0.05$; ** $P < 0.01$; *** $P < 0.001$.

with nontransgenic littermates (N = 5) (**Fig. 9A**). Conversely, ABCG1-deficient mice showed significantly decreased SREBP-2 mRNA levels and a clear trend toward lower HMG-CoAR mRNA levels (N = 7) (Fig. 9B). These findings suggest that SREBP-2-dependent feedback regulation of sterol biosynthesis is responsive to ABCG1-mediated changes in sterol precursor levels in vivo.

DISCUSSION

Several lines of evidence support a role for LXR-responsive genes in the pathogenesis of AD. Many studies have now demonstrated that synthetic LXR agonists reduce Aβ levels in vivo, and improve cognitive function in mouse models of AD (61–64). Conversely, deficiency of LXRα and LXRβ each leads to greater amyloid and Aβ burden in APP/PS1 mice (61). Identifying the gene or genes that mediate the beneficial properties of LXR agonists could have significant therapeutic relevance. The primary purpose of this study was therefore to determine whether ABCG1 may have in vivo roles in AD pathogenesis by regulating Aβ metabolism, amyloid neuropathology, or apoE levels.

ABCG1 is one of several genes upregulated by synthetic LXR agonists and is highly expressed in brain. Genetic studies suggest a possible role for ABCG1 in Aβ metabolism, as different single nucleotide polymorphism haplotypes show either an increased or decreased odds ratio for AD risk in two European populations (80). Support for a potential role for ABCG1 in APP processing was recently provided by Tansley et al. (52), who observed that ABCG1 overexpression increased Aβ production 30% and increased APP processing through α- and β-secretase in HEK-APP cells. However, Kim et al. (56) observed the opposite finding in CHO-APP cells, where excess ABCG1 was associated with a 60% reduction in Aβ secretion. Because ABCG1 participates in the regulation of cellular cholesterol homeostasis, and APP processing is markedly influenced by the levels and distribution of intracellular cholesterol, these disparate in vitro findings highlight the importance of evaluating ABCG1 function in AD pathogenesis in an in vivo model system.

To test the hypothesis that ABCG1 affects AD pathogenesis, we generated a BAC-Tg animal model expressing functional human ABCG1 from its endogenous regulatory sequences. ABCG1-BAC-Tg mice overexpress LXR-responsive ABCG1 in both neurons and glia, and exhibit a 6-fold increase in ABCG1 protein in both cortex and hippocampus. However, excess ABCG1 in PDAPP mice led to only marginal increases in soluble Aβ42 in young ABCG1-overexpressing animals, which was not maintained by 1 year of age. Furthermore, excess ABCG1 did not affect soluble Aβ40, or deposited Aβ40 or Aβ42, at any age. Consistent with these observations, C99 levels and Aβ-mediated deficits in learning and memory also remained unchanged in ABCG1 overexpressing mice both prior to and during early stages of amyloid deposition. We also expanded the scope of our analysis to encompass ABCG1 deficiency by determining endogenous mAβ levels in *Abcg1* hemizygous and knockout animals. Although mAβ40 levels were significantly reduced in *Abcg1* hemizygous mice, there was no change in Aβ40 in ABCG1-deficient animals, or any change in mAβ42 in mice lacking one or both copies of the *Abcg1* gene. Therefore, although it is possible that excess ABCG1 may have a subtle influ-

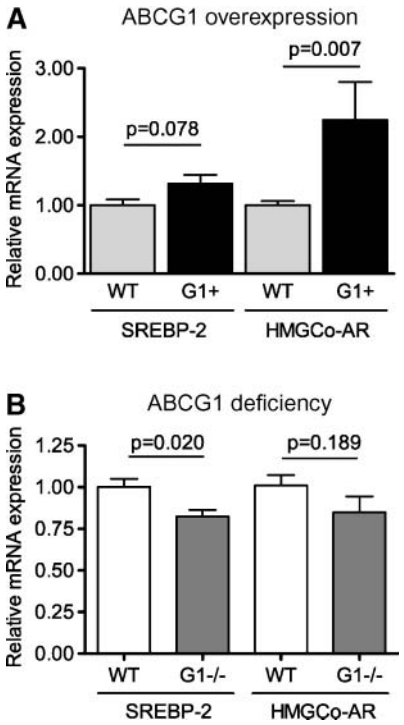

Fig. 9. ABCG1 gene dose is associated with altered SREBP-2 and HMG-CoA-reductase (HMG-CoAR) mRNA levels. mRNA levels of SREBP-2 and HMG-CoAR were determined by QRT-PCR analysis of RNA extracted from whole brain of (A) adult wild-type (WT, N = 5) and ABCG1-BAC-Tg (G1+, N = 5) mice, as well as (B) wild-type homozygous ($^{-/-}$, N = 7) and ABCG1-deficient (N = 7) animals. Statistical analysis was by unpaired Student's *t*-test. Error bars indicate ± SEM.

ence on soluble Aβ42 levels in early disease, neither deficiency nor overexpression of ABCG1 appears to have biologically significant effects on deposited Aβ levels or amyloid burden. Finally, we found that ABCA1 and apoE levels were unaffected by ABCG1 overexpression or deficiency.

Our results clearly demonstrate that ABCG1 does not participate in the metabolism of Aβ, apoE, or ABCA1 in vivo in a manner that significantly impacts AD pathogenesis. Possible explanations for the discrepancies between the in vitro and in vivo findings could be explained by the degree of overexpression achieved in cultured cells compared with that in transgenic animals, and the presence of other physiologic variables such as clearance of Aβ from the brain through transporters such as LRP or p-glycoprotein, or proteolytic degradation of excess Aβ by insulin-degrading enzyme or neprilysin.

We conclude from these studies that the beneficial effects of LXR agonists on AD pathogenesis are unlikely to be due to ABCG1. Rather, we propose that ABCA1, a related cholesterol transporter also highly induced by LXR agonists, may be a prime candidate. We and others have identified ABCA1 as a key regulator of apoE levels and lipidation in vivo, which affects Aβ and amyloid metabolism in several independent mouse models of AD (13–16, 60, 63). Although low levels of ABCA1 overexpression in a BAC-Tg animal model were insufficient to affect Aβ and amyloid levels (72), robust overexpression of ABCA1 in brain has recently been determined to attenuate Aβ and amyloid deposition in PDAPP mice (77). These observations provide strong support for the role of ABCA1 as a major beneficial LXR target gene for AD, although the effects of combined ABCA1 and ABCG1 overexpression remain to be determined.

ABCG1 does, however, appear to influence brain cholesterol metabolism in vivo. Overexpression of ABCG1 was associated with decreased levels of sterol intermediates and 24OH-cholesterol in brain, whereas progressive inactivation of ABCG1 alleles resulted in a corresponding increase in sterol intermediates as well as 24OH-cholesterol levels in a gene dose-responsive manner, similar to results recently reported by Wang et al. (53). These data suggest that functional ABCG1 may have a role in regulating the cholesterol biosynthetic pathway, and are consistent with the recent observations of Kennedy et al. who reported a global upregulation of HMG-CoAR, HMG synthase and farnesyl-pyrophosphate synthase, and SREBP-1c in liver of *Abcg1*-deficient animals on a chow diet (43), as well as those by Tarr and Edwards (54),who recently reported that ABCG1 affects SREBP-2 processing, which in turn influences the expression of SREBP-2-resposive genes in the CNS. HMG-CoA is the first step in the biosynthesis of both isoprenoid and cholesterol, and inhibition of isoprenoid synthesis affects both inflammatory responses and the neuronal signaling required for LTP. Indeed, cyp46-deficient mice have greatly reduced brain cholesterol biosynthesis, are profoundly impaired in learning and memory tasks, and exhibit no LTP in electrophysiological studies (7). Although the total mass of brain cholesterol is unchanged in either *Abgc1*-deficient or -overexpressing brain, this probably reflects compensatory changes in *Cyp46*-mediated elimination of cholesterol through 24S-hydroxycholesterol, because 24OH-cholesterol levels change in parallel with sterol intermediates. Tight homeostatic regulation of brain cholesterol metabolism is reported by Thelen et al. (81), who confirm that pharmacological inhibition of cholesterol synthesis in the brain reduces cholesterol turnover through 24S-hydroxycholesterol but not total cholesterol levels. Conversely, mice deficient for cyp46 cannot clear excess cholesterol through 24S-hydroxycholesterol yet are observed to have an almost complete inhibition of HMG-CoAR while retaining normal levels of total cholesterol (6). It is important to note that because 70–80% of free cholesterol in the brain is sequestered in myelin, small changes in membrane cholesterol levels may be difficult to detect but may have large effects on neuronal function (1).

This study demonstrates that neither 6-fold excess of ABCG1 nor complete ablation of ABCG1 are associated with robust changes in Aβ levels in vivo. These findings suggest that it is highly unlikely that ABCG1 contributes to the beneficial effects of LXR agonists on amyloid pathology or Aβ-mediated cognitive impairments, at least in the absence of concomitant ABCA1 overexpression. The failure to replicate either of the findings from the two reports on ABCG1 and Aβ secretion in cultured cells

reinforces the need to interpret the results of cell-based Aβ metabolism studies with caution. Notably, however, this study also demonstrates that ABCG1 activity may participate in the regulation of cholesterol biosynthesis in the CNS. ABCG1 activity is associated with reduced levels of sterol intermediates in vivo and is associated with elevated SREBP-2 and HMG-CoAR mRNAs. Conversely, deficiency of ABCG1 results in increased sterol intermediates in vivo and reduced SREBP-2 and HMG-CoAR mRNA levels. These observations lend additional support for the function of ABCG1 as a regulator of cholesterol homeostasis in brain and other body tissues.

The authors are grateful to the members of their research teams for invaluable discussions throughout the course of this work.

REFERENCES

1. Dietschy, J. M., and S. D. Turley. 2001. Cholesterol metabolism in the brain. *Curr. Opin. Lipidol.* **12:** 105–112.
2. Poirier, J. 1994. Apolipoprotein E in animal models of CNS injury and Alzheimer's disease. *Trends Neurosci.* **17:** 525–530.
3. Mahley, R. W., and S. C. Rall, Jr. 2000. Apolipoprotein E: far more than a lipid transport protein. *Annu. Rev. Genomics Hum. Genet.* **1:** 507–537.
4. Lund, E. G., T. A. Kerr, J. Sakai, W. P. Li, and D. W. Russell. 1998. cDNA cloning of mouse and human cholesterol 25-hydroxylases, polytopic membrane proteins that synthesize a potent oxysterol regulator of lipid metabolism. *J. Biol. Chem.* **273:** 34316–34327.
5. Lund, E. G., J. M. Guileyardo, and D. W. Russell. 1999. cDNA cloning of cholesterol 24-hydroxylase, a mediator of cholesterol homeostasis in the brain. *Proc. Natl. Acad. Sci. USA.* **96:** 7238–7243.
6. Lund, E. G., C. Xie, T. Kotti, S. D. Turley, J. M. Dietschy, and D. W. Russell. 2003. Knockout of the cholesterol 24-hydroxylase gene in mice reveals a brain-specific mechanism of cholesterol turnover. *J. Biol. Chem.* **278:** 22980–22988.
7. Kotti, T. J., D. M. O. Ramirez, B. E. Pfeiffer, K. M. Huber, and D. W. Russell. 2006. Brain cholesterol turnover required for geranylgeraniol production and learning in mice. *Proc. Natl. Acad. Sci. USA.* **103:** 3869–3874.
8. Wolozin, B. 2004. Cholesterol and the biology of Alzheimer's disease. *Neuron.* **41:** 7–10.
9. Corder, E. H., A. M. Saunders, W. J. Strittmatter, D. E. Schmechel, P. C. Gaskell, G. W. Small, A. D. Roses, J. L. Haines, and M. A. Pericak-Vance. 1993. Gene dose of apolipoprotein E type 4 and the risk of Alzheimer's disease in late onset families. *Science.* **261:** 921–923.
10. Corder, E. H., A. M. Saunders, N. J. Risch, W. J. Strittmatter, D. E. Schmechel, P. C. Gaskell, J. B. Rimmler, P. A. Locke, P. M. Conneally, K. E. Schmader, et al. 1994. Protective effect of apolipoprotein E type 2 for late onset Alzheimer disease. *Nat. Genet.* **7:** 180–184.
11. Poirier, J., J. Davignon, D. Bouthillier, S. Kogan, P. Bertrand, and S. Gauthier. 1993. Apolipoprotein E polymorphism and Alzheimer's disease. *Lancet.* **342:** 697–699.
12. Price, D. L., R. E. Tanzi, D. R. Borchelt, and S. S. Sisodia. 1998. Alzheimer's disease: genetic studies and transgenic models. *Annu. Rev. Genet.* **32:** 461–493.
13. Hirsch-Reinshagen, V., S. Zhou, B. L. Burgess, L. Bernier, S. A. McIsaac, J. Y. Chan, G. H. Tansley, J. S. Cohn, M. R. Hayden, and C. L. Wellington. 2004. Deficiency of ABCA1 impairs apolipoprotein E metabolism in brain. *J. Biol. Chem.* **279:** 41197–41207.
14. Wahrle, S. E., H. Jiang, M. Parsadanian, J. Legleiter, X. Han, J. D. Fryer, T. Kowalewski, and D. M. Holtzman. 2004. ABCA1 is required for normal CNS apoE levels and for lipidation of astrocyte-secreted apoE. *J. Biol. Chem.* **279:** 40987–40993.
15. Hirsch-Reinshagen, V., L. F. Maia, B. L. Burgess, J. F. Blain, K. E. Naus, S. A. McIsaac, P. F. Parkinson, J. Y. Chan, G. H. Tansley, M. R. Hayden, et al. 2005. The absence of ABCA1 decreases soluble apoE levels but does not diminish amyloid deposition in two murine models of Alzheimer disease. *J. Biol. Chem.* **280:** 43243–43256.
16. Wahrle, S., H. Jiang, M. Parsadanian, R. E. Hartman, K. R. Bales, S. M. Paul, and D. M. Holtzman. 2005. Deletion of Abca1 increases Abeta deposition in the PDAPP transgenic mouse model of Alzheimer disease. *J. Biol. Chem.* **280:** 43236–43242.
17. Koldamova, R., M. Staufenbiel, and I. Lefterov. 2005. Lack of ABCA1 considerably decreases brain apoE level and increases amyloid deposition in APP23 mice. *J. Biol. Chem.* **280:** 43224–43235.
18. Wahrle, S. E., A. R. Shah, A. M. Fagan, S. Smemo, J. S. Kauwe, A. Grupe, A. Hinrichs, K. Mayo, H. Jiang, L. J. Thai, et al. 2007. Apolipoprotein E levels in cerebrospinal fluid and the effects of ABCA1 polymorphisms. *Mol Neurodegener.* **12:** 2–7.
19. Hartmann, T. 2001. Cholesterol, Aβ and Alzheimer's disease. *Trends Neurosci.* **24 (Suppl.):** 45–48.
20. Haass, C., and D. J. Selkoe. 1993. Cellular processing of β-amyloid precursor and the genesis of amyloid β-peptide. *Cell.* **75:** 154–159.
21. Vassar, R., B. D. Bennett, S. Babu-Khan, S. Kahn, E. A. Mendiaz, P. Denis, D. B. Teplow, S. Ross, P. Amarante, R. Loeloff, et al. 1999. β-Secretase cleavage of Alzheimer's amyloid precursor protein by the transmembrane aspartic protease BACE. *Science.* **286:** 735–741.
22. Ehehalt, R., P. Keller, C. Haass, C. Thiele, and K. Simons. 2003. Amyloidogenic processing of the Alzheimer β-amyloid precursor protein depends on lipid rafts. *J. Cell Biol.* **160:** 113–123.
23. Kimberley, W. T., M. J. LaVoie, B. L. Ostaszeski, W. Ye, M. S. Wolfe, and D. J. Selkoe. 2003. γ-Secretase is a membrane protein complex comprised of presenilin, nicastrin, aph-1, and pen-2. *Proc. Natl. Acad. Sci. USA.* **100:** 6382–6387.
24. Kojro, E., G. Gimple, S. Lammich, W. März, and F. Fahrenholz. 2001. Low cholesterol stimulates the nonamyloidogenic pathway by its effect on the α-secretase ADAM 10. *Proc. Natl. Acad. Sci. USA.* **98:** 5815–5820.
25. Lammich, S., E. Kojro, R. Postina, S. Gilbert, R. Pfeiffer, M. Jasionowski, C. Haass, and F. Fahrenholz. 1999. Constitutive and regulated α-secretase cleavage of Alzheimer's amyloid precursor protein by a disintegrin metalloprotease. *Proc. Natl. Acad. Sci. USA.* **96:** 3922–3927.
26. Buxbaum, J. D., K. N. Liu, Y. Luo, J. L. Slack, K. L. Stocking, J. J. Peschon, R. S. Johnson, B. J. Castner, D. P. Cerretti, and R. A. Black. 1998. Evidence that tumor necrosis factor α converting enzyme is involved in regulated α-secretase cleavage of the Alzheimer amyloid protein precursor. *J. Biol. Chem.* **273:** 27765–27767.
27. Refolo, L. M., M. A. Pappolla, B. Malester, J. LaFrancois, T. Bryant-Thomas, R. Wang, G. S. Tint, K. Sambamurti, and K. Duff. 2000. Hypercholesterolemia accelerates the Alzheimer's amyloid pathology in a transgenic mouse model. *Neurobiol. Dis.* **7:** 321–331.
28. Shie, F. S., L. W. Jin, D. G. Cook, J. B. Leverenz, and R. C. LeBoeuf. 2002. Diet-induced hypercholesterolemia enhances brain A beta accumulation in transgenic mice. *Neuroreport.* **213:** 455–459.
29. Wahrle, S., P. Das, A. C. Nyborg, C. McLendon, M. Shoji, T. Kawarabayashi, L. H. Younkin, S. G. Younkin, and T. E. Golde. 2002. Cholesterol-dependent γ-secretase activity in buoyant cholesterol-rich membrane microdomains. *Neurobiol. Dis.* **9:** 11–23.
30. Burns, M., K. Gaynor, V. Olm, M. Mercken, J. LaFrancois, L. Wang, P. M. Matthews, W. Noble, Y. Matsuoka, and K. Duff. 2003. Presenilin redistribution associated with aberrant cholesterol transport enhances β-amyloid production in vivo. *J. Neurosci.* **23:** 5645–5649.
31. Fassbender, K., M. Simons, C. Bergmann, M. Stroick, D. Lütjohann, P. Keller, H. Runz, S. Kühl, T. Bertsch, K. von Bergmann, et al. 2001. Simvastatin strongly reduces levels of Alzheimer's disease β-amyloid peptides Aβ42 and Aβ40 in vitro and in vivo. *Proc. Natl. Acad. Sci. USA.* **98:** 5856–5861.
32. Simons, M., P. Keller, B. De Strooper, K. Beyreuther, C. G. Dottie, and K. Simons. 1998. Cholesterol depletion inhibits the generation of β-amyloid in hippocampal neurons. *Proc. Natl. Acad. Sci. USA.* **95:** 6460–6464.
33. Bodovitz, S., and W. L. Klein. 1996. Cholesterol modulates α-secretase cleavage of amyloid precursor protein. *J. Biol. Chem.* **271:** 4436–4440.
34. Buxbaum, J. D., N. S. Geoghagan, and L. T. Friedhoff. 2001. Cholesterol depletion with physiological concentrations of a statin decreases the formation of the Alzheimer amyloid Abeta peptide. *J. Alzheimers Dis.* **3:** 221–229.

35. Schmitz, G., T. Langmann, and S. Heimerl. 2001. Role of ABCG1 and other ABCG family members in lipid metabolism. *J. Lipid Res.* **42:** 1513–1520.
36. Cavelier, C., I. Lorenzi, L. Rohrer, and A. von Eckardstein. 2006. Lipid efflux by the ATP-binding cassette transporters ABCA1 and ABCG1. *Biochim. Biophys. Acta.* **1761:** 655–666.
37. Vaughan, A. M., and J. F. Oram. 2005. ABCG1 redistributes cell cholesterol to domains removable by HDL but not by lipid-depleted apolipoproteins. *J. Biol. Chem.* **280:** 30150–30157.
38. Wang, N., M. Ranalletta, F. Matsuura, F. Peng, and A. Tall. 2006. LXR-induced redistribution of ABCG1 to plasma membrane in macrophages enhances cholesterol mass efflux to HDL. *Arterioscler. Thromb. Vasc. Biol.* **26:** 1310–1316.
39. Kobayashi, A., Y. Takanezawa, T. Hirata, Y. Shimizu, K. Misasa, N. Kioka, H. Arai, K. Ueda, and M. Matsuo. 2006. Efflux of sphingomyelin, cholesterol, and phosphatidylcholine by ABCG1. *J. Lipid Res.* **47:** 1791–1802.
40. Terasaka, N., N. Wang, L. Yvan-Charvet, and A. R. Tall. 2007. High-density lipoprotein protects macrophages from oxidized low-density lipoprotein-induced apoptosis by promoting efflux of 7-ketocholesterol via ABCG1. *Proc. Natl. Acad. Sci. USA.* **104:** 15093–15098.
41. Gelissen, I. C., M. Harris, K-A. Rye, C. Quinn, A. J. Brown, M. Kockx, S. Cartland, M. Packianthan, L. Kritharides, and W. Jessup. 2006. ABCA1 and ABCG1 synergize to mediate cholesterol export to apoA-1. *Arterioscler. Thromb. Vasc. Biol.* **26:** 534–540.
42. Vaughan, A. M., and J. F. Oram. 2006. ABCA1 and ABCG1 or ABCG4 act sequentially to remove cellular cholesterol and generate cholesterol-rich HDL. *J. Lipid Res.* **47:** 2433–2443.
43. Kennedy, M. A., G. C. Barrera, K. Nakamura, A. Baldán, P. Tarr, M. C. Fishbein, J. Frank, O. L. Francone, and P. A. Edwards. 2005. ABCG1 has a critical role in mediating cholesterol efflux to HDL and preventing cellular lipid accumulation. *Cell Metab.* **1:** 121–131.
44. Baldán, A., P. Tarr, C. S. Vales, J. Frank, T. K. Shimotake, S. Hawgood, and P. A. Edwards. 2006. Deletion of the transmembrane transporter ABCG1 results in progressive pulmonary lipidosis. *J Biol Chem.* **281:** 29401–29410.
45. Baldán, A., L. Pei, R. Lee, P. Tarr, R. K. Tangirala, M. M. Weinstein, J. Frank, A. C. Li, P. Tontonoz, and P. A. Edwards. 2006. Impaired development of atherosclerosis in hyperlipidemic Ldlr−/− and ApoE−/− mice transplanted with Abcg1−/− bone marrow. *Arterioscler. Thromb. Vasc. Biol.* **26:** 2301–2307.
46. Out, R., M. Hoekstra, R. B. Hildebrand, J. K. Kruit, I. Meurs, Z. Li, F. Kuipers, T. J. Van Berkel, and M. Van Eck. 2006. Macrophage ABCG1 deletion disrupts lipid homeostasis in alveolar macrophages and moderately influences atherosclerotic lesion development in LDL receptor-deficient mice. *Arterioscler. Thromb. Vasc. Biol.* **26:** 2295–2300.
47. Out, R., M. Hoekstra, I. Meurs, P. de Vos, J. Kuiper, M. Van Eck, and T. J. Van Berkel. 2007. Total body ABCG1 expression protects against early atherosclerotic lesion development in mice. *Arterioscler. Thromb. Vasc. Biol.* **27:** 594–599.
48. Ranalletta, M., N. Wang, S. Han, L. Yvan-Charvet, C. Welch, and A. R. Tall. 2006. Decreased atherosclerosis in low-density lipoprotein receptor knockout mice transplanted with Abcg1−/− bone marrow. *Arterioscler. Thromb. Vasc. Biol.* **26:** 2308–2315.
49. Buchmann, J., C. Meyer, S. Neschen, R. Augustin, K. Schmolz, R. Kluge, H. Al-Hasani, H. Jürgens, K. Eulenberg, R. Wehr, et al. 2006. Ablation of the cholesterol transporter adenosine triphosphate-binding cassette transporter G1 reduces adipose cell size and protects against diet-induced obesity. *Endocrinology.* **148:** 1561–1573.
50. Curtiss, L. K. 2006. Is two out of three enough for ABCG1? *Arterioscler. Thromb. Vasc. Biol.* **26:** 2175–2177.
51. Basso, F., M. J. Amar, E. M. Wagner, B. Vaisman, B. Paigen, S. Santamarina-Fojo, and A. T. Remaley. 2006. Enhanced ABCG1 expression increases atherosclerosis in LDLr-KO mice on a western diet. *Biochem. Biophys. Res. Commun.* **351:** 398–404.
52. Tansley, G. H., B. L. Burgess, M. T. Bryan, Y. Su, V. Hirsch-Reinshagen, J. Pearce, J. Y. Chan, A. Wilkinson, J. Evans, K. E. Naus, et al. 2007. The cholesterol transporter ABCG1 modulates the subcellular distribution and proteolytic processing of β-amyloid precursor protein. *J. Lipid Res.* **48:** 1022–1034.
53. Wang, N., L. Yvan-Charvet, D. Lutjohann, M. Mulder, T. Vanmierlo, T. W. Kim, and A. R. Tall. ATP-binding cassette transporters G1 and G4 mediate cholesterol and desmosterol efflux to HDL and regulate sterol accumulation in the brain. *FASEB J.* Epub ahead of print. November 26, 2007; doi:
54. Tarr, P. T., and P. A. Edwards. 2007. ABCG1 and ABCG4 are co-expressed in neurons and astrocytes of the CNS and regulate cholesterol homeostasis through SREBP-2. *J. Lipid Res.* **49:** 169–182.
55. Karten, B., R. B. Campenot, D. E. Vance, and J. E. Vance. 2006. Expression of ABCG1, but not ABCA1, correlates with cholesterol release by cerebellar astroglia. *J. Biol. Chem.* **281:** 4049–4057.
56. Kim, W. S., A. S. Rahmanto, A. Kamili, K. A. Rye, G. J. Guillemin, I. C. Gelissen, W. Jessup, A. F. Hill, and B. Garner. 2006. Role of ABCG1 and ABCA1 in regulation of neuronal cholesterol efflux to apolipoprotein-E discs and suppression of amyloid-β peptide generation. *J. Biol. Chem.* **282:** 2851–2861.
57. Fukumoto, H., A. Deng, M. C. Irizarry, M. L. Fitzgerald, and G. W. Rebeck. 2002. Induction of the cholesterol transporter ABCA1 in CNS cells by LXR agonists increases secreted Aβ levels. *J. Biol. Chem.* **277:** 48508–48513.
58. Koldamova, R. P., I. M. Lefterov, M. D. Ikonomovic, J. Skoko, P. I. Lefterov, B. A. Isanski, S. T. DeKosky, and J. S. Lazo. 2003. 22R-hydroxycholesterol and 9-cis-retinoic acid induce ATP-binding cassette transporter A1 expression and cholesterol efflux in brain cells and decrease amyloid β secretion. *J. Biol. Chem.* **278:** 13244–13256.
59. Sun, Y., J. Yao, T-W. Kim, and A. R. Tall. 2003. Expression of LXR target genes decreases cellular amyloid β peptide secretion. *J. Biol. Chem.* **278:** 27688–27694.
60. Burns, M. P., L. Vardanian, A. Pajoohesh-Gangi, L. Wang, M. Cooper, D. C. Harris, K. Duff, and G. W. Rebeck. 2006. The effects of ABCA1 on cholesterol efflux and Aβ levels in vitro and in vivo. *J. Neurochem.* **98:** 792–800.
61. Zelcer, N., N. Khanlou, R. Clare, Q. Jiang, E. G. Reed-Geaghan, G. E. Landreth, H. V. Vinters, and P. Tontonoz. 2007. Attenuation of neuroinflammation and Alzheimer's disease pathology by liver X receptors. *Proc. Natl. Acad. Sci. USA.* **104:** 10601–10606.
62. Lefterov, I., A. L. Bookout, Z. Wang, M. Staufenbiel, D. J. Mangelsdorf, and R. Koldamova. Expression profiling in APP23 mouse brain: inhibition of Abeta amyloidosis and inflammation in response to LXR agonist treatment. *Mol Neurodegener.* Epub ahead of print. October 22, 2007.
63. Koldamova, R. P., I. M. Lefterov, M. Staufenbiel, D. Wolfe, S. Huang, J. C. Glorioso, M. Walter, M. G. Roth, and J. S. Lazo. 2005. The liver X receptor ligand TO901317 decreases amyloid β production in vitro and in a mouse model of Alzheimer's disease. *J. Biol. Chem.* **280:** 4079–4088.
64. Riddell, D. R., H. Zhou, T. A. Comery, E. Kouranova, C. F. Lo, H. K. Warwick, R. H. Ring, Y. Kirksey, S. Aschmies, J. Xu, et al. 2007. The LXR agonist TO901317 selectively lowers hippocampal Aβ42 and improves memory in the Tg2576 mouse model of Alzheimer's disease. *Mol. Cell. Neurosci.* **34:** 621–628.
65. Games, D., D. Adams, R. Alessandrini, R. Barbour, P. Berthelette, C. Blackwell, T. Carr, J. Clemens, T. Donaldson, F. Gillespie, et al. 1995. Alzheimer-type neuropatholgoy in transgenic mice overexpressing V717F β-amyloid precursor protein. *Nature.* **373:** 523–527.
66. DeMattos, R. B., K. R. Bales, M. Parsadanian, M. A. O'Dell, E. M. Foss, S. M. Paul, and D. M. Holtzman. 2002. Plaque-associated disruption of CSF and plasma amyloid-β (Aβ) equilibrium in a mouse model of Alzheimer's disease. *J. Neurochem.* **81:** 229–236.
67. Albrecht, C., S. Soumian, J. S. Amey, A. Sardini, C. F. Higgins, A. H. Davies, and R. G. Gibbs. 2004. ABCA1 expression in carotid atherosclerotic plaques. *Stroke.* **35:** 2801–2806.
68. Wellington, C. L., E. K. Walker, A. Suarez, A. Kwok, N. Bissada, R. Singaraja, Y-Z. Yang, L. H. Zhang, E. James, J. E. Wilson, et al. 2002. ABCA1 mRNA and protein distribution patterns predict multiple different roles and levels of regulation. *Lab. Invest.* **82:** 273–283.
69. DeMattos, R. B., J. R. Cirrito, M. Parsadanian, P. C. May, M. A. O'Dell, J. W. Taylor, J. A. Harmony, B. J. Aronow, K. R. Bales, S. M. Paul, et al. 2004. ApoE and clusterin cooperatively suppress Aβ levels and deposition: evidence that apoE regulates extracellular Aβ metabolism in vivo. *Neuron.* **41:** 193–202.
70. Lutjohann, D., A. Brzezinka, E. Barth, D. Abramowski, M. Staufenbiel, K. von Bergmann, K. Beyreuther, G. Multhaup, and T. A. Bayer. 2002. Profile of cholesterol-related sterols in aged amyloid precursor protein transgenic mouse brain. *J. Lipid Res.* **43:** 1078–1085.
71. Lutjohann, D., O. Breuer, G. Ahlborg, L. Nennesmo, A. Siden, U. Diczfalusy, and I. Bjorkhem. 1996. Cholesterol homeostasis in human brain: evidence for an age-dependent flux of 24S-hydroxycholesterol from the brain into the circulation. *Proc. Natl. Acad. Sci. USA.* **93:** 9799–9804.

72. Hirsch-Reinshagen, V., J. Y. Chan, A. Wilkinson, T. Tanaka, J. Fan, G. Ou, L. F. Maia, R. Singaraja, M. R. Hayden, and C. L. Wellington. 2007. Physiologically regulated ABCA1 does not reduce amyloid burden or beta-amyloid levels in vivo. *J. Lipid Res.* **48:** 914–923.
73. von Eckardstein, A., M. Hersberger, and L. Rohrer. 2005. Current understanding of the metabolism and biological actions of HDL. *Curr. Opin. Clin. Nutr. Metab. Care.* **8:** 147–152.
74. Hartman, R. E., Y. Izumi, K. R. Bales, S. M. Paul, D. F. Wozniak, and D. M. Holtzman. 2005. Treatment with an amyloid-beta antibody ameliorates plaque load, learning deficits, and hippocampal long-term potentiation in a mouse model of Alzheimer's disease. *J. Neurosci.* **25:** 6213–6220.
75. Bales, K. R., T. Verina, R. Dodel, Y. Du, L. Alsteil, M. Bender, P. Hyslop, E. M. Johnstone, S. P. Little, D. J. Cummins, et al. 1997. Lack of apolipoprotein E dramatically reduces amyloid beta-peptide deposition. *Nat. Genet.* **17:** 263–264.
76. Bell, R. D., A. P. Sagaare, A. E. Friedman, G. S. Bedi, D. M. Holtzman, R. Deane, and B. V. Zlokovic. 2006. Transport pathways for clearance of human Alzheimer's amyloid β-peptide and apolipoproteins E and J in the mouse central nervous system. *J. Cereb. Blood Flow Metab.* **27:** 909–918.
77. Wahrle, S. E., H. Jiang, M. Parsadanian, J. Kim, A. Li, A. Knoten, S. Jain, V. Hirsch-Reinshagen, C. L. Wellington, K. R. Bales, et al. 2008. Overexpression of ABCA1 reduces amyloid deposition in the PDAPP mouse model of Alzheimer disease. *J. Clin. Invest.* **118:** 671–682.
78. von Eckardstein, A., C. Langer, T. Engel, I. Schaukal, A. Cignarella, J. Reinhardt, S. Lorkowski, Z. Li, X. Zhou, P. Cullen, et al. 2001. ATP binding cassette transporter ABCA1 modulates the secretion of apolipoprotein E from human monocyte-derived macrophages. *FASEB J.* **15:** 1555–1561.
79. Lutjohann, D., K. von Bergmann, H. Bardenheuer, T. Hartmann, K. von Bergmann, K. Beyreuther, and J. Schröder. 2002. Cerebrospinal fluid 24S-hydroxycholesterol is increased in patients with Alzheimer's disease compared to healthy controls. *Neurosci. Lett.* **324:** 83–85.
80. Wollmer, M. A., J. R. Streffner, M. Tsolaki, L. M. E. Grimaldi, D. Lutjohann, D. Thal, K. von Bergmann, R. M. Nitsch, and A. Papassotiropoulos. 2003. Genetic association of acyl-coenzyme A: cholesterol acyltransferase with cerebrospinal fluid cholesterol levels, brain amyloid load, and risk for Alzheimer's disease. *Mol. Psychiatry.* **8:** 635–638.
81. Thelen, K. M., K. M. Rentsch, U. Gutteck, M. Heverin, M. Olin, U. Andersson, E. A. von Eckardstein, I. Bjorkhem, and D. Lutjohann. 2006. Brain cholesterol synthesis in mice is affected by high dose of simvastatin but not of pravastatin. *J. Pharmacol. Exp. Ther.* **316:** 1146–1152.